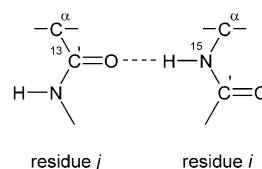


## Direct Observation of Intramolecular Hydrogen Bonds in Peptide $3_{10}$ Helices by $^3J_{N,C'}$ Scalar Couplings

Massimo Bellanda, Mario Rainaldi,  
 Quirinus B. Broxterman, Bernard Kaptein,  
 Fernando Formaggio, Marco Crisma, Stefano Mammi,  
 and Claudio Toniolo\*

In a recent series of papers, Grzesiek and co-workers reported the observation of cross hydrogen-bond  $^{15}\text{N}$ – $^{13}\text{C}'$  scalar couplings ( $^3J_{N,C'}$ ) in proteins characterized by  $\alpha$ -helix and  $\beta$ -sheet conformations.<sup>[1]</sup> This coupling establishes an electron-mediated connection between the amide nitrogen and carbonyl carbon nuclei of two amino acid residues involved in an intramolecular  $\text{C}=\text{O}\cdots\text{H}-\text{N}$  hydrogen bond (see schematic representation). The discovery of this spin–spin cou-



pling phenomenon between nuclei across hydrogen bonds offers an important new tool to unequivocally determine the donor and the acceptor (the latter is particularly difficult to identify) of a hydrogen bond in isotopically enriched biomolecules. Other groups have recently published significant theoretical and experimental papers on this methodology by examining  $\alpha$ -helix and  $\beta$ -sheet proteins.<sup>[2]</sup> Direct evidence for a central  $\alpha$ -helical region in the peptaibol chrysospermin C in micelles was obtained by using this approach.<sup>[3]</sup>

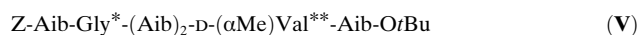
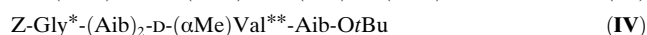
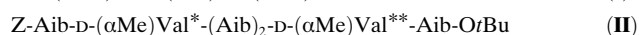
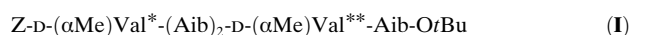
The principal limitation for a successful detection of these very weak correlations stems from the low sensitivity of the related NMR spectroscopic experiments. Detection of the weak  $^3J_{N,C'}$  couplings relies on the use of long de- and rephasing intervals. For large proteins, the sensitivity of this long-range H(N)CO experiment rapidly decreases because of  $^{15}\text{N}$  transverse-relaxation losses during the extended magnetization-transfer periods. Although the absolute size of the  $^3J_{N,C'}$  couplings is small, it is possible to trace out nearly

[\*] Dr. M. Bellanda, Dr. M. Rainaldi, Prof. F. Formaggio, Dr. M. Crisma, Prof. S. Mammi, Prof. C. Toniolo  
 Department of Chemistry, University of Padova  
 and CNR ICB, Padova Unit  
 via Marzolo 1, 35131 Padova (Italy)  
 Fax: (+39) 049-827-5139  
 E-mail: claudio.toniolo@unipd.it  
 Dr. Q. B. Broxterman, Dr. B. Kaptein  
 DSM Pharma Chemicals,  
 Advanced Synthesis and Catalysis  
 P.O. Box 18, 6160 MD, Geleen (The Netherlands)

Supporting information for this article is available on the WWW under <http://www.angewandte.org> or from the author.

complete hydrogen-bond networks in small, nondeuterated proteins ( $\leq 10$ kDa) by using the long-range H(N)CO method. An improvement in sensitivity can be obtained by quenching the scalar-coupling-mediated relaxation by using an adiabatic or a composite pulse decoupling on the aliphatic carbon atoms<sup>[4]</sup> or, for larger proteins, by the TROSY approach<sup>[1b,5]</sup> and deuteration. In the small protein ubiquitin,  $^3\text{h}J_{\text{N,C}}$  coupling constants down to 0.1 Hz have been detected.<sup>[1a]</sup> More recently, Jaravine et al.<sup>[1d]</sup> showed the applicability of this method to a marginally stable  $\alpha$ -helical peptide and demonstrated that the size of the individual  $^3\text{h}J_{\text{N,C}}$  coupling constants can be used as a measure of the population of the helical conformation.

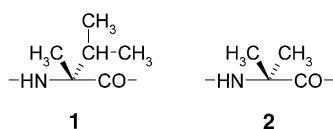
Hydrogen-bond correlations in ubiquitin have been observed for almost all hydrogen bonds in the  $\alpha$  helix as well as in the various  $\beta$  sheets, but none of the hydrogen bonds in  $3_{10}$ -helices seen in the crystal and NMR spectroscopically derived structures of ubiquitin give rise to observable correlations. Apparently, the failure to detect  $^3\text{h}J_{\text{N,C}}$  couplings in the  $3_{10}$ -helices of ubiquitin stems from an unfavorable geometry for the hydrogen bonds.<sup>[2g]</sup> In the present work, we measured the very small  $^3\text{h}J_{\text{N,C}}$  couplings in  $3_{10}$ -helices for the first time. To this end, we synthesized the series of short peptides **I–V**, which contain, in addition to Gly, the



(Z = benzyloxycarbonyl; \* =  $^{13}\text{C}$  =O-labeled residue;

\*\* =  $^{15}\text{N}$ -H-labeled residue)

$\text{C}^\alpha$ -tetrasubstituted  $\alpha$ -amino acid residues D-( $\alpha$ Me)Val (**1**;  $\text{C}^\alpha$ -methyl-D-valine) and Aib (**2**;  $\alpha$ -aminoisobutyric acid).



These penta- and hexapeptides were designed to fold in stable (left-handed)  $3_{10}$  helices, by taking advantage of the predominant presence of D-( $\alpha$ Me)Val and Aib residues,<sup>[6]</sup> and to incorporate selectively  $^{13}\text{C}$ - and  $^{15}\text{N}$ -labeled residues at appropriate positions suitable for monitoring helical C=O $\cdots$ H-N hydrogen bonds. More specifically, the limited main-chain length ( $< 8$  residues) of the peptides and the 80–100% occurrence of  $\text{C}^\alpha$ -tetrasubstituted residues in their sequences are known to favor strongly the onset of a  $3_{10}$  helix over an  $\alpha$  helix.<sup>[6]</sup> In any case, hexapeptide **III**, with its two consecutive  $^{13}\text{C}$ =O-labeled residues, was tailored to distinguish between these two types of helical structures. The incorporation of a flexible Gly residue at the N-terminus (pentapeptide **IV**) or near the N-terminus (hexapeptide **V**) was expected to provide information on fraying of the helical end.

The X-ray diffraction structure of the terminally protected pentapeptide **I** represented unambiguous experimental proof

of the conformational preference of the above peptides for the  $3_{10}$  helix in the crystal state (Figure 1). The molecules are indeed found in a regular, left-handed,  $3_{10}$ -helical structure (from residues 1 to 4). The C-terminal Aib residue is helical

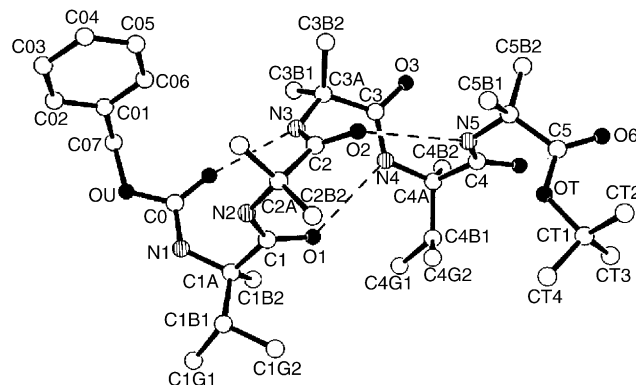


**Figure 1.** X-ray diffraction structure of the terminally protected, left-handed,  $3_{10}$ -helical pentapeptide **I** with atom numbering. The three C=O $\cdots$ H-N intramolecular hydrogen bonds are represented by dashed lines.

too, but the signs of the  $\phi, \psi$  torsion angles are opposite to those exhibited by the preceding residues (a common observation for  $3_{10}$ -helical peptide esters).<sup>[6a]</sup> The average  $\phi, \psi$  torsion angles for the four left-handed helical residues are  $+54.9^\circ, +28.7^\circ$ , which are close to the values expected for a  $3_{10}$  helix.<sup>[7]</sup> Three consecutive C=O $\cdots$ H-N intramolecular hydrogen bonds of the  $i \leftarrow i + 3$  type stabilize the helical structure (N3-H3 $\cdots$ O0=C0, N4-H4 $\cdots$ O1=C1 and N5-H5 $\cdots$ O2=C2). The corresponding N $\cdots$ O distances are 3.183(3), 3.003(3), and 3.107(3) Å, and the N-H $\cdots$ O angles are 158.5, 170.6, and 167.3 $^\circ$ , respectively.

The FTIR absorption spectra in the N-H stretching region of all five peptides in solution ( $\text{CDCl}_3$ ;  $c = 1$  mM), in which self-association is absent (not shown), are similar and characterized by two bands. As an example, Figure 2 illustrates the spectrum of pentapeptide **I**. The weak absorption at  $\sim 3430$   $\text{cm}^{-1}$  is assigned to free, solvated NH groups and the stronger absorption at  $\sim 3345$   $\text{cm}^{-1}$  to hydrogen-bonded NH groups.<sup>[8a,b]</sup> These curves are typical of helical peptides. In addition, the ratios of the integrated molar extinction coefficients for the hydrogen-bonded and free NH groups of the five peptides fall nicely on the curve of these ratios as a function of the number of peptide units in  $3_{10}$ -helical peptides, as recently reported and discussed by Pispisa et al.<sup>[8c]</sup> These FTIR absorption results provided firm and independent evidence that the  $3_{10}$ -helical structure preferred in the crystalline state by the ( $\alpha$ Me)Val- and Aib-rich peptides is also largely populated in noncompeting solvents.

For the detection of the  $J$  coupling across the hydrogen bond between the donor  $^{15}\text{N}$  and the acceptor carbonyl  $^{13}\text{C}$ , a 2D version of the pulse scheme proposed by Cordier and Grzesiek<sup>[1a]</sup> was used, in which the chemical shift evolution of the  $^{15}\text{N}$  nucleus was not recorded. The sensitivity required to detect very small coupling constants was achieved for several reasons. First, the peptides examined have a strong tendency to fold in stable  $3_{10}$  helices. More importantly, as they are very

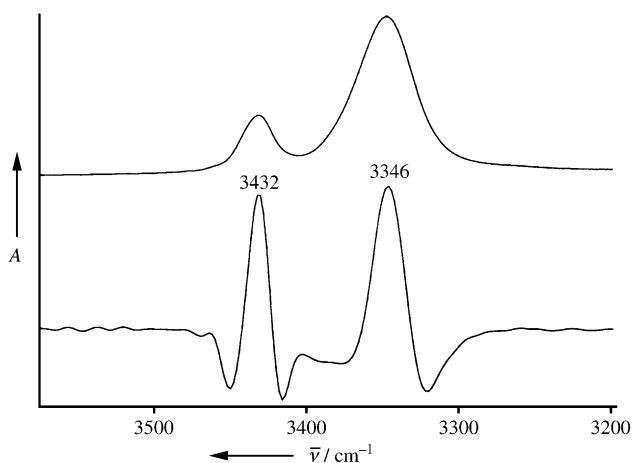


**Figure 2.** FTIR absorption and inverted second derivative spectra (3550–3200  $\text{cm}^{-1}$  region) of the terminally protected pentapeptide **I** in  $\text{CDCl}_3$  ( $c = 1 \text{ mM}$ ).

soluble in MeOH, concentrations in the order of 10 mM were easily obtained. This was a key factor, because the chance to observe a cross-peak increases very slowly with the number of scans, making the use of high concentrations often the only possibility to detect small couplings. Furthermore,  $^{15}\text{N}$  transverse-relaxation losses decrease owing to the very small size of the peptides and the scalar-coupling-mediated relaxation is negligible because the aliphatic carbon atoms are present at natural abundance. Considering a detection limit of three times the standard deviation of the noise obtained in the different experiments, couplings down to 0.03–0.04 Hz could be detected. The portions of the spectra showing the correlations of interest are shown in Figure 3.

The size of the long-range coupling was determined from the measured intensity ratio for the correlation  $^{15}\text{N}_i, ^{13}\text{C}_j$  in the long-range experiment ( $I_{\text{lr}}$ ) relative to the  $^{15}\text{N}_i, ^{13}\text{C}_{i+1}$  correlation in the reference experiment ( $I_{\text{ref}}$ ). The implicit equation for  $I_{\text{lr}}/I_{\text{ref}}$  described by Cordier and Grzesiek<sup>[1a]</sup> was solved by numerical inversion. This equation requires a knowledge of the  $^1J_{\text{N}_i\text{C}_{i+1}}$  values, which cannot be determined easily with high accuracy with our labeling scheme. Therefore, the equation was solved with  $^1J_{\text{N}_i\text{C}_{i+1}} = 15.6 \text{ Hz}$ , a value in the middle of the range reported for the  $3_{10}$ -helical segment in ubiquitin (15.1–16.1 Hz).<sup>[9]</sup> A different choice would not produce very different results. Even considering the full range of couplings measured in ubiquitin (13.5–17.2 Hz), the calculated  $^3hJ_{\text{N}_i\text{C}_j}$  values would differ less than 0.02 Hz from those reported in Figure 3. The uncertainty in  $^1J_{\text{N}_i\text{C}_{i+1}}$  is the main source of error in  $^3hJ_{\text{N}_i\text{C}_j}$ . When three standard deviations of the noise are used as the statistical error for the experimental intensities, the error propagation on the simplified formula proposed in reference [1a] leads to much smaller errors in  $^3hJ_{\text{N}_i\text{C}_j}$ . The role of the  $^2J_{\text{N}_i\text{C}_i}$  passive coupling in the experimental error was considered to be negligible because the carbonyl group of the residue containing the  $^{15}\text{N}$  amide is not isotopically enriched, and the values of this constant are small anyway.

With the exception of peptide **IV**, a signal indicating the presence of a hydrogen bond typical of the  $3_{10}$  helix between

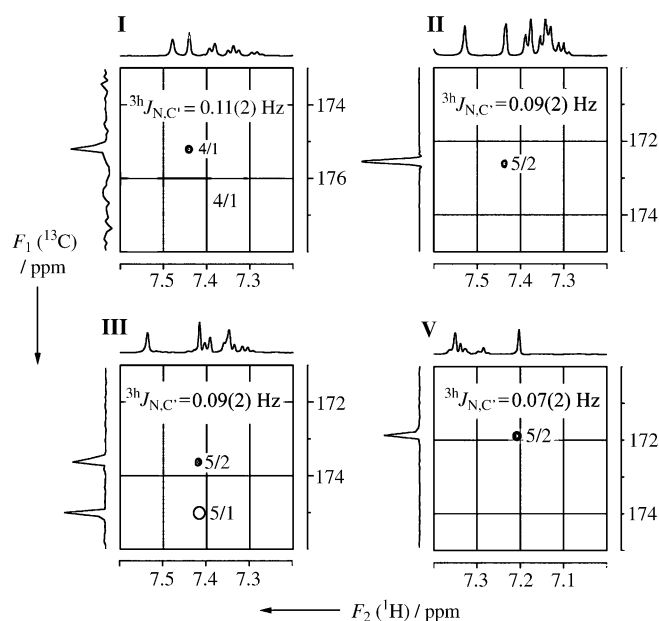


**Figure 3.** Portions of the long-range 2D H(N)CO spectra of the terminally protected peptides **I**, **II**, **III**, and **V** in  $\text{CD}_3\text{OH}$  ( $c = 10 \text{ mM}$ ). Peaks are marked by the residue number of the donor N–H group followed by the residue number of the acceptor carbonyl group. In each spectrum, the value of  $^3hJ_{\text{N}_i\text{C}_j}$  is also indicated. The error in these values was estimated to be lower than 0.02 Hz. For peptide **III**, in which two  $^{13}\text{C}$ -labeled ( $\alpha\text{Me}$ )Val residues are present, resonances of the two N-terminal amino acids were assigned by combination of a ROESY experiment and an HMBC experiment (not shown). The area of the spectrum where the  $(i+4)^{15}\text{N}-(i)^{13}\text{C}$  scalar coupling was expected, is indicated by an empty circle.

labeled C=O and N–H groups was always observed. The measured  $^3hJ_{\text{N}_i\text{C}_j}$  values (Figure 3) are significantly lower than those recorded for  $\alpha$ -helical peptides, as expected from the less-than-optimal hydrogen-bond geometry in  $3_{10}$  helices.

For peptide **IV**, which contains a Gly residue at the N-terminus, it was not possible to observe any signal above the detection limit, probably because of the high mobility of this protein residue. When an Aib residue was added at the N-terminus (peptide **V**), the peak corresponding to the hydrogen bond between Gly<sup>2</sup> and ( $\alpha\text{Me}$ )Val<sup>5</sup> was clearly observed, although the slightly lower value of  $^3hJ_{\text{N}_i\text{C}_j}$  might indicate that some fraying is still present. Finally, in peptide **III**, designed to allow direct detection of the hydrogen bond for both the  $3_{10}$ - and the  $\alpha$ -helical structures, only the signal indicating the presence of the  $3_{10}$  helix was seen, unequivocally demonstrating the propensity of these short peptides for such a type of helical folding. From our data, the presence of a small population of  $\alpha$ -helical peptides cannot be excluded. Based on the fact that the detection limit for this particular experiment is 0.03 Hz and that the average value found for the  $^3hJ_{\text{N}_i\text{C}_j}$  constants in  $\alpha$ -helical hydrogen bonds of the fully folded ubiquitin is  $0.38 \pm 0.12 \text{ Hz}$ ,<sup>[1a]</sup> an  $\alpha$ -helix population of less than about 10% would not be observable.

In summary, we have determined the correlation between the  $^{13}\text{C}$ -labeled ( $i$ ) carbonyl group and the hydrogen-bonded proton of the  $^{15}\text{N}$ -labeled ( $i+3$ ) NH group for five short  $3_{10}$ -helical peptides. The magnetization transfer is achieved by

$^3J_{\text{N,C}}$  scalar coupling through the hydrogen bond in an H(N)CO-type experiment. Interestingly, in MeOH, a solvent compatible with peptide helical structures, this phenomenon is clearly seen with peptides **I**, **II**, **III** and **V**, but not with peptide **IV**, most probably because the labeled carbonyl residue (Gly) in the latter is quite flexible and located at the beginning of the main chain (N-terminal fraying). Of the five peptides, only pentapeptide **IV** does not bear a conformationally restricted C $^{\alpha}$ -tetrasubstituted  $\alpha$ -amino acid at the N-terminus. This study is the first successful application of this novel and important NMR spectroscopic methodology to  $3_{10}$ -helical peptides. It is also noteworthy that in peptide **III** the  $^{15}\text{N}$ - $^{13}\text{C}$  scalar coupling between the (*i*) ( $\alpha$ Me)Val carbonyl carbon atom and the (*i*+4) ( $\alpha$ Me)Val amide nitrogen atom is not seen, allowing us to conclude that the  $\alpha$ -helical structure is essentially absent in this hexapeptide. This finding demonstrates the power of this technique to discriminate between the two most relevant helical structures ( $\alpha$  vs.  $3_{10}$ ) in peptides and proteins. However, our results indicate that detection of intramolecular C=O...H-N hydrogen bonds in  $3_{10}$  helices by  $^3J_{\text{N,C}}$  scalar couplings is feasible only when peptide segments are conformationally rigidified.

### Experimental Section

Preparation of unlabeled and  $^{15}\text{N}$ -H- or  $^{13}\text{C}$ =O-labeled, enantiopure C $^{\alpha}$ -methyl-D-valines was performed by DSM Pharma Chemicals.<sup>[10]</sup> Terminally protected peptides were synthesized step by step in solution, beginning from the C-terminus. These sterically demanding peptide bonds were formed in moderate to good yields either by the *N*-ethyl, *N'*-[(3-(dimethylamino)propyl)carbodiimide/7-aza-1-hydroxy-1,2,3-benzotriazole]<sup>[11a]</sup> or by the acyl fluoride<sup>[11b]</sup> C-activation method. For details of the synthesis and characterization of the five final peptides and their synthetic intermediates, see Supporting Information.

IR absorption: The solution IR absorption spectra were recorded on a Perkin-Elmer model 1720 X FTIR spectrometer. Spectrograde CDCl<sub>3</sub> (99.8%) was purchased from Aldrich.

NMR: The H(N)CO type experiments were carried out at 298 K, in CD<sub>3</sub>OH on a Bruker Avance 600 instrument. Each spectrum results from 80(t1) × 1024(t2) complex data points and was recorded with 480 scans. The reference spectrum was acquired with the same parameters in an interleaved way, and the total measuring time for each pair of spectra was 56 h.

X-Ray diffraction: The data were collected on a Philips PW1100 four-circle diffractometer. Single crystals suitable for X-ray diffraction analysis were grown from ethyl acetate/petroleum ether by vapor diffusion.<sup>[12]</sup>

Received: March 9, 2004 [Z54224]

**Keywords:** helical structures · IR spectroscopy · NMR spectroscopy · peptides · X-ray diffraction

- [1] a) F. Cordier, S. Grzesiek, *J. Am. Chem. Soc.* **1999**, *121*, 1601; b) Y.-X. Wang, J. Jacob, F. Cordier, P. Wingfield, S. J. Stahl, S. Lee-Huang, D. Torchia, S. Grzesiek, A. Bax, *J. Biomol. NMR* **1999**, *14*, 181; c) A. J. Dingley, F. Cordier, S. Grzesiek, *Concepts Magn. Reson.* **2001**, *13*, 103; d) V. A. Jaravine, A. T. Alexandrescu, S. Grzesiek, *Protein Sci.* **2001**, *10*, 943; e) F. Cordier, S. Grzesiek, *J. Mol. Biol.* **2002**, *317*, 739.
- [2] a) G. Cornilescu, J.-S. Hu, A. Bax, *J. Am. Chem. Soc.* **1999**, *121*, 2949; b) G. Cornilescu, B. E. Ramirez, M. K. Frank, G. M. Clore,

- A. M. Gronenborn, A. Bax, *J. Am. Chem. Soc.* **1999**, *121*, 6275; c) M. Barfield, *J. Am. Chem. Soc.* **2002**, *124*, 4158; d) A. Bagno, *Chem. Eur. J.* **2000**, *6*, 2925; e) C. Scheurer, R. Bruschweiler, *J. Am. Chem. Soc.* **1999**, *121*, 8661; f) N. Juranic, S. Macura, *J. Am. Chem. Soc.* **2001**, *123*, 4099; g) N. Juranic, M. C. Moncrieffe, V. A. Likic, F. G. Prendergast, S. Macura, *J. Am. Chem. Soc.* **2002**, *124*, 14221; h) C. M. Bougault, M. K. Eidgness, J. H. Prestegard, *Biochemistry* **2003**, *42*, 4357; i) W. D. Arnold, E. Oldfield, *J. Am. Chem. Soc.* **2000**, *122*, 12835; j) P. R. L. Markwick, R. Sprangers, M. Sattler, *J. Am. Chem. Soc.* **2003**, *125*, 644; k) T. Tuttle, J. Gräfenstein, A. Wu, E. Kraka, D. Cremer, *J. Phys. Chem. B* **2004**, *108*, 1115; l) G. Gemmecker, *Angew. Chem.* **2000**, *112*, 1276; *Angew. Chem. Int. Ed.* **2000**, *39*, 1224.
- [3] R. Anders, O. Ohlenschläger, V. Soskic, H. Wenschuh, B. Heise, L. R. Brown, *Eur. J. Biochem.* **2000**, *267*, 1784.
- [4] A. Liu, W. Hu, S. Qamar, A. Majumdar, *J. Biomol. NMR* **2000**, *17*, 55.
- [5] K. Pervushin, R. Riek, G. Wider, K. Wüthrich, *Proc. Natl. Acad. Sci. USA* **1997**, *94*, 12366.
- [6] a) C. Toniolo, M. Crisma, F. Formaggio, C. Peggion, *Biopolymers* **2001**, *60*, 396; b) I. L. Karle, P. Balaram, *Biochemistry* **1990**, *29*, 6747.
- [7] a) C. Toniolo, E. Benedetti, *Trends Biochem. Sci.* **1991**, *16*, 350; b) K. A. Bolin, G. L. Millhauser, *Acc. Chem. Res.* **1999**, *32*, 1027.
- [8] a) M. T. Cung, M. Marraud, J. Néel, *Ann. Chim. (Paris)* **1972**, *183*; b) G. M. Bonora, C. Mapelli, C. Toniolo, R. R. Wilkenson, E. S. Stevens, *Int. J. Biol. Macromol.* **1984**, *6*, 179; c) B. Pispisa, A. Palleschi, L. Stella, M. Venanzi, C. Mazzuca, F. Formaggio, C. Toniolo, Q. B. Broxterman, *J. Phys. Chem. B* **2002**, *106*, 5733.
- [9] N. Juranic, P. K. Ilich, S. Macura, *J. Am. Chem. Soc.* **1995**, *117*, 405.
- [10] a) W. H. Kruizinga, J. Bolster, R. M. Kellogg, J. Kamphuis, W. H. J. Boesten, E. M. Meijer, H. E. Schoemaker, *J. Org. Chem.* **1988**, *53*, 1826; b) B. Kaptein, W. H. J. Boesten, Q. B. Broxterman, P. J. H. Peters, H. E. Schoemaker, J. Kamphuis, *Tetrahedron: Asymmetry* **1993**, *4*, 1113.
- [11] a) L. A. Carpino, *J. Am. Chem. Soc.* **1993**, *115*, 4397; b) L. A. Carpino, E. S. M. E. Mansour, D. Sadat-Aalae, *J. Org. Chem.* **1991**, *56*, 2611.
- [12] Crystal-structure determination of **I** (C<sub>36</sub>H<sub>59</sub>N<sub>5</sub>O<sub>8</sub>): crystal dimensions 0.5 × 0.2 × 0.2 mm<sup>3</sup>; orthorhombic, *P*2<sub>1</sub>2<sub>1</sub>2<sub>1</sub>; *a* = 11.710(3) Å, *b* = 16.319(4) Å, *c* = 21.269(5) Å; *V* = 4064.4(17) Å<sup>3</sup>;  $\rho_{\text{calcd}}$  = 1.127 Mg m<sup>-3</sup>;  $2\theta_{\text{max}}$  = 120°; Cu<sub>K $\alpha$</sub>  radiation ( $\lambda$  = 1.54178 Å),  $\theta$ - $2\theta$  scan mode, *T* = 293 K; 3750 collected reflections, 3702 of which were independent; *h*, *k*, *l* limits:  $-1 \leq h \leq 13$ ,  $0 \leq k \leq 18$ ,  $0 \leq l \leq 23$ . Intensities were corrected for Lorentz and polarization effects, not for absorption ( $\mu$  = 0.647 cm<sup>-1</sup>). The structure was solved by direct methods by using the SIR 2002 program,<sup>[13a]</sup> and anisotropically refined by full-matrix block least-squares on *F*<sup>2</sup> by application of the SHELXL 97<sup>[13b]</sup> program. Data/restraints/parameters: 3702/1/430. Hydrogen atoms were calculated at idealized positions and refined as riding. *R*<sub>1</sub> = 0.047 [on *F* ≥ 4σ(*F*)]; *wR*<sub>2</sub> = 0.148 (on *F*<sup>2</sup>, all data). Max./min. residual electron density peaks: +0.512/−0.229 e Å<sup>-3</sup>. CCDC 230-250 contains the supplementary crystallographic data for this paper. These data can be obtained free of charge via [www.ccdc.cam.ac.uk/conts/retrieving.html](http://www.ccdc.cam.ac.uk/conts/retrieving.html) (or from the Cambridge Crystallographic Data Centre, 12, Union Road, Cambridge CB2 1EZ, UK; fax: (+44)1223-336-033; or deposit@ccdc.cam.ac.uk).
- [13] a) M. C. Burla, M. Camalli, B. Carrozzini, G. L. Cascarano, C. Giacovazzo, G. Polidori, R. Spagna, *J. Appl. Crystallogr.* **2003**, *36*, 1103; b) G. M. Sheldrick, *SHELXL-97 Program for Crystal Structure Refinement*, University of Göttingen, Göttingen, Germany, **1997**.